Early Specification of the Hierarchical Organization of Visual Cortical Areas in the Macaque Monkey

Alexandre Batardière, Pascal Barone[2], Kenneth Knoblauch, Pascale Giroud, Michel Berland[1], Anne-Marie Dumas[1] and Henry Kennedy

Cerveau et Vision INSERM 371, 18 Avenue du Doyen Lépine, 69675 Bron Cedex and [1]Faculté de Médecine Lyon Sud, Service de Gynécologie Obstétrique, Centre Hospitalier Lyon Sud, 165 Chemin du Grand Revoyet, 69495 Pierre Bénite Cedex, France [2]Current address: Centre de Recherche Cerveau et Cognition, CNRS–UPS–UMR 5549, Université Paul Sabatier, 133 route de Narbonne, 31062 Toulouse Cedex, France

The laminar organization of cortico-cortical projection neurons (expressed by the percentage of supragranular projecting neurons – SLN%) characterizes cortical pathways as feedforward (FF) or feedback (FB) and determines the hierarchical ranking of cortical areas. There is evidence of a developmental reduction in SLN% of pathways to area V1. Here, by analyzing pre- and postnatal projections to area V4, we have been able to address whether developmental reductions of SLN% impact on information processing in the immature cortex. FB pathways to area V4 exhibit 28–84% reduction of SLN%. This contrasts with the FF projections, which show little or no SLN% reduction. However, SLN% values in the immature cortex allocated cortical areas to the same hierarchical levels as in the adult. The developmental reduction of SLN% is a widespread phenomenon in the neocortex and is a distinctive feature of FB pathways. Two mechanisms contribute to developmental changes in SLN%: (i) delayed ingrowth of axons into the cortical target from infragranular layer neurons and (ii) prolonged developmental reduction of the divergence of projections from supragranular layer neurons. The present results show that FF and FB projections exhibit different developmental processes and patterns of connections linking cortical areas and their hierarchical relations are established prenatally, independently of regressive phenomena.

Introduction

Hierarchical organization of information processing in the brain has been an important issue in neurology since the work of Huglins Jackson in the1880s. The work of Hubel and Wiesel formalized the relevance of hierarchical processing for understanding both the physiology and the connectivity of the visual system (Hubel and Wiesel, 1962). More recently, a number of conceptually important studies have used mathematical treatment of connectivity data to address the hierarchical organization of the cortex using various combinations of graph theory and non-metric multidimensional scaling (Young, 1992; Jouve *et al.*, 1998; Hilgetag *et al.*, 2000; Sporns *et al.*, 2000).

Laminar Patterns of Cortical Connectivity

Rostral directed projections allow outflow of activity away from striate cortex (area V1) towards circumstriate cortex and are thought of as feedforward (FF) pathways. These projections originate largely from supragranular layers, target layer 4 and contrast with the reciprocal, caudal directed projections which in the main originate in infragranular layers, terminate outside of layer 4 and are thought of as feedback (FB) pathways (Lund *et al.*, 1975; Rockland and Pandya, 1979; Maunsell and Van Essen, 1983; Kennedy and Bullier, 1985; Barbas, 1986; Boussaoud *et al.*, 1990; Morel and Bullier, 1990; Webster *et al.*, 1991; Distler *et al.*, 1993; Barone *et al.*, 1995, 2000; Barbas and Rempel Clower, 1997; Felleman *et al.*, 1997b; Gattass *et al.*, 1997; Rempel Clower and Barbas, 2000).

Definitions of Hierarchical Organization, Hierarchical Distance and Hierarchical Rank

The laminar patterns of cortico-cortical connections indicate an anatomical hierarchical ranking of primate cortical areas. For a given cortical area, higher-order areas have FB relations and lower-order areas have FF relations. Pairwise comparisons of the laminar patterns of connectivity have made it possible to determine the hierarchical organization of the visual system which places area V1, V2, V3, etc. on successive hierarchical levels (Maunsell and Van Essen, 1983; Ungerleider and Desimone, 1986; Boussaoud *et al.*, 1990; Felleman and Van Essen, 1991; Webster *et al.*, 1991, 1994; Young, 1992; Distler *et al.*, 1993; Rockland 1997; Barone *et al.*, 2000; Hilgetag *et al.*, 2000).

Individual cortico-cortical pathways exhibit a precise laminar distribution of the parent neurons characterized by the percentage of labeled supragranular layer neurons – SLN%, see Figure 1 (Barone *et al.*, 2000). Following injections of tracers in area V4, SLN% increases at successive lower hierarchical levels, so the SLN% is 60% in area V3, 93% in V2 and 100% in V1. Conversely, there is a progressive decrease in SLN% at successive higher levels. In this way the value of SLN% relates to the number of hierarchical levels separating two cortical areas, which we refer to as the hierarchical distance (Fig. 1). This makes SLN% values extremely powerful in generating hierarchical models of the visual cortex (Barone *et al.*, 2000).

Experimental Aims of the Present Study

During pre- and postnatal development, all cortical areas which project to area V1 show a 45–90% reduction in SLN% values (Kennedy *et al.*, 1989; Barone *et al.*, 1995). This raises a number of issues concerning the development of association pathways linking cortical areas which we have investigated in the present study.

Firstly, the developmental reduction of the SLN% of area V1 afferents occurs during a period when there is an overall reduction in numbers of connections. This raises the possibility that selective elimination of connections creates the characteristic SLN% differences between areas.

Secondly, by shaping inter-areal connectivity, selective elimination during development could modify the hierarchical organization of the cortex, which in turn might imply differences in the physiological function of the immature cortex (Dehay *et al.*, 1988).

Thirdly, the developmental remodeling of connections might be restricted to projections to area V1, given that this area exhibits a number of unique features (Dehay *et al.*, 1988; Dehay and Kennedy, 1993). Remodeling could be a developmental feature of cortical projections to primary areas, which supposedly receive FF input uniquely via their afferents from the principal thalamic relay nuclei.

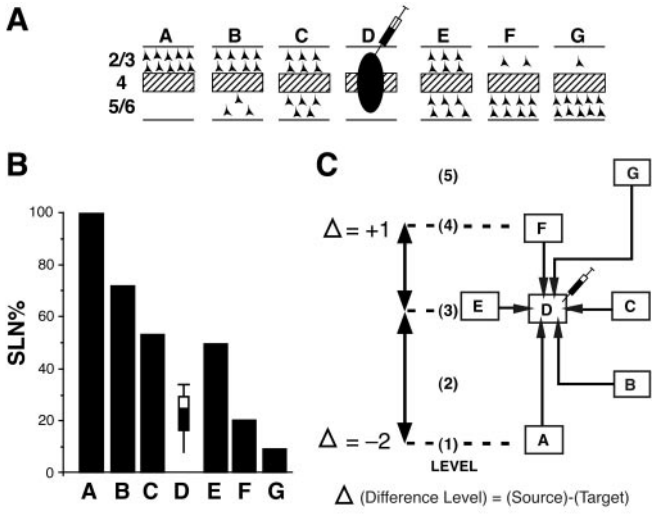

Figure 1. Definition of hierarchical modal, rank and distance. (*A*) Injection of retrograde tracer in area D makes it possible to determine the hierarchical relationship of afferent areas. As one moves upstream (i.e. to areas at lower hierarchical ranks), there is a progressive increase in the percentage of labeled supragranular projection neurons (SLN%). Moving in a downstream direction leads to a progressive decrease in SLN%. (*B*) Counts of labeled neurons throughout the projection zone make it possible to obtain highly reproducible SLN% values for each area. (*C*) For each pathway it is possible to calculate the number of hierarchical levels separating two areas. In this example, areas C and E have SLN% values near to 50% and are considered to be lateral connections. Areas B and D have progressively higher percentages and are located on levels 2 and 1, respectively. The number of levels separating area D on level 3 and A on level 1 is –2, which corresponds to a high SLN%. Conversely, the number of levels separating area G on level 5 and D on level 3 is +2, which corresponds to a low SLN%. Because the projections from areas G and A cross two levels, this corresponds to a larger hierarchical distance than that separating area D from areas F and B. In this way, the relative configuration of areas corresponds to the hierarchical model of these areas, the rank is the level to which each area is assigned and the distance is the number of levels separating two given areas. Barone *et al*. give further details (Barone *et al*., 2000).

Fourthly, earlier studies of the development of projections to area V1 provide no information as to whether there is a developmental remodeling of FF projections. This requires investigating the connectivity of a cortical area such as area V4, which receives both FF and FB cortico-cortical connections.

To address these issues, we have examined the connectivity of the visual area V4 using a method for determining the laminar distribution of projection neurons, which is immune to developmental changes in density.

Materials and Methods

Anesthesia and Surgery

Retrograde tracer experiments were carried out on cynomolgus monkeys, *Macaca fascicularis* (Table 1). Following premedication with atropine (1.25 mg, i.m.) and dexamethasone (4 mg, i.m.), monkeys were prepared for surgery under ketamine hydrochloride (20 mg/kg, i.m.) and chlorpromazine (2 mg/kg, i.m.). In the case of fetal surgery, the pregnant monkey was premedicated in a similar fashion to the postnatal animals, with the addition of isoxsuprine (2.5 mg i.m.). After intubation, anesthesia was continued with 1% halothane in N_2O/O_2 (70/30). Heart rate was monitored and respiration adjusted to maintain the end-tidal CO_2 at 4.5–6%. The rectal temperature was maintained at 37°C. In the pregnant monkey, a midline abdominal incision allowed uterotomy to be performed over the posterior part of the fetal brain.

Injection of Retrograde Tracers

Stereotyped injections (3–5 mm) of retrograde fluorescent tracers

Table 1
Experimental cases

Case	Age at injection	Survival time	Dye
BB 115	E 106	9	Fb
BB 109	E 112	11	Fb[a]
BB 130	E 123	11	Fb[a]–DY
BB 131	E 140	11	Fb[a]–DY
BB 127	PND 6	13	Fb[a]–DY
BB187	PND 59	13	Fb–DY
BB119	PND 61	12	Fb–DY
BB135	PNM 13	11	Fb
M72	Adult	12	Fb–DY

Abbreviations: E, embryonic day; PND, post-natal day; PNM, post-natal month; Fb, fast blue; DY, dyamidino yellow.

[a]Injections that involve the subplate.

(0.5–1.5 µl; 3% in H_20) were made by means of Hamilton syringes on the prelunate gyrus between the LS the IOS and the STS, in area V4 containing the representation of the central visual field (Gattass *et al*., 1988). Injection sites spanned the full thickness of the cortex – cortical depth of injection does not influence SLN%, as found previously (Barone *et al*., 1994; Batardière *et al*., 1998a) and in the present study (data not shown). Elsewhere, we have characterized the uptake zone of Fb and DY tracers (Kennedy and Bullier, 1985) and reconstructions of injection sites (Fig. 2) showed that of the 15 injections, 11 were successfully confined to the cortical gray matter of presumptive area V4. In three of the fetal injections, the uptake zone extended into the subplate (Kostovic and Rakic, 1990; Smart *et al*., 2002). In one injection in the newborn, the injection contaminated the underlying white matter (Table 1). For prenatal material, the fetus was replaced in the uterus and incisions were closed using routine procedures. The pregnant monkey received postoperative medication consisting of a muscular relaxant (isoxsuprine chlorydrate) and an analgesic (tiemonium methylsulfate).

Histological Processing

Fetuses were delivered by Caesarean section after a 9–13 day survival period. Animals were deeply anaesthetized with a lethal dose of pentobarbital (i.p.) before being perfused transcardially with 200 ml of 2.7% saline, 1–3 l of 8% paraformaldehyde/0.5% glutaraldehyde mixture in phosphate buffer (0.1 M, pH = 7.4), 0.5 l 10% sucrose, 0.5 l 20% sucrose and 1 l 30% sucrose in phosphate buffer (0.1 M, pH = 7.4). Brains were immediately removed, blocked and horizontal 40 m thick sections cut on a freezing microtome. One section in three was mounted in saline onto gelatinized slides. Sections at regular intervals were reacted for cytochrome oxidase activity (Silverman and Tootell, 1987) and acetylcholinesterase activity (Mesulam and Geula, 1994).

Examination of Material

Sections were observed in UV light with oil-immersion objectives using a Leitz fluorescent microscope equipped with a D-filter set (355–425 nm). Neurons labeled by DY exhibit a yellow nucleus, while neurons labeled by Fb exhibit a blue coloration in their cytoplasm. An *x*–*y* plotter electronically coupled to the microscope stage was used to trace out sections and to record the positions of labeled neurons. After observation, sections were counterstained with cresyl violet and projected on to charts of labeled neurons so as to relate the positions of labeled neurons to histological borders.

Areal and Laminar Distribution of Labeled Neurons

At all ages, injection of tracers into area V4 leads to dense labeling of an extensive region of extrastriate cortex in the occipital, parietal and temporal regions (Tanaka *et al*., 1990; Baizer *et al*., 1991; Felleman and Van Essen, 1991; Shipp and Zeki, 1995; Barone *et al*., 2000), in different known visual areas (V2, V3A, MT, FST, LIP, FEF, TEO, TE) and in TH/TF (Fig. 2*D*). The areal extent of a population of retrogradely labeled neurons in one cortical area resulting from an injection in the target area is referred to as a projection zone.

The laminar distribution was expressed as the percentage of labeled supragranular layer neurons with respect to the overall population of

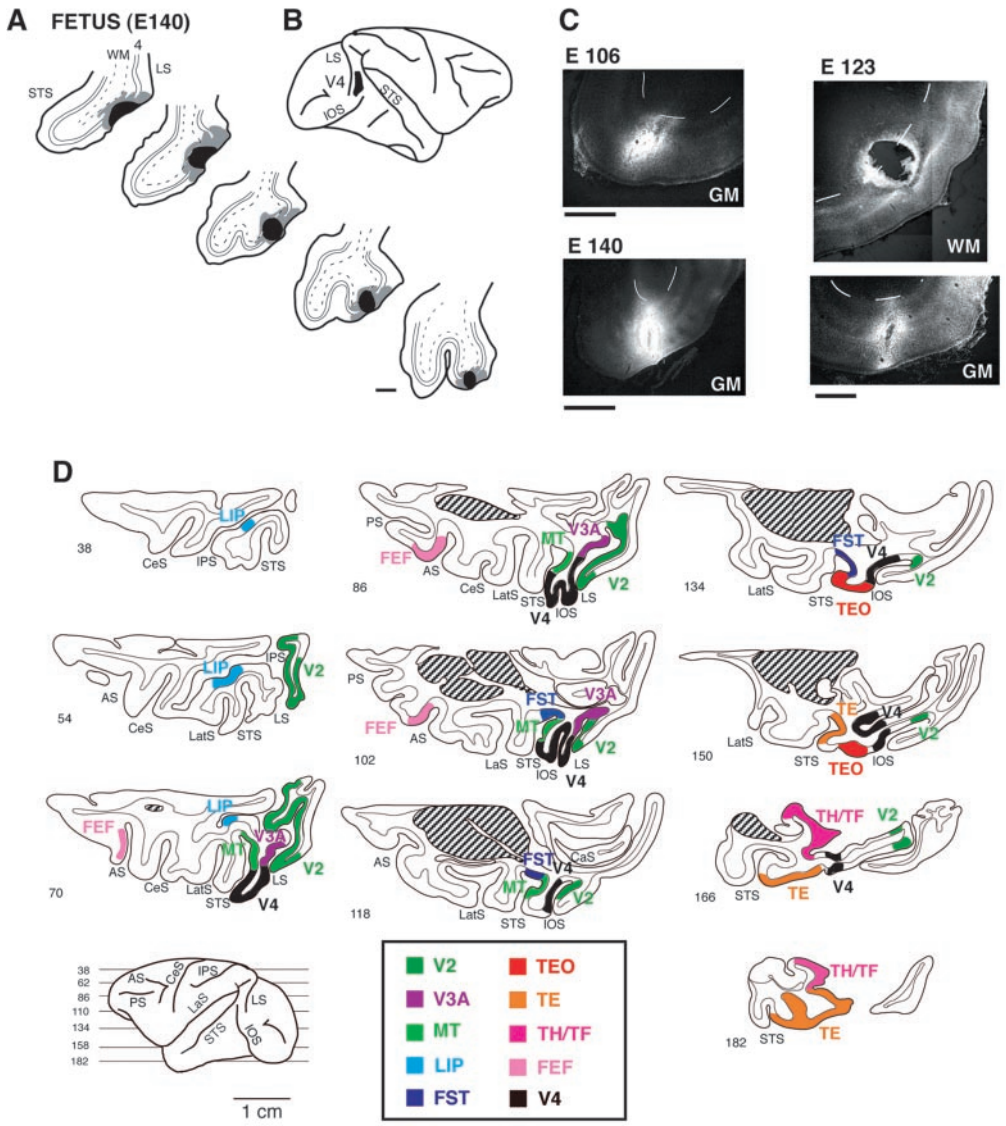

Figure 2. Injection sites and areal extent of labeling. (*A*) Fb injection site in the E140 fetus. The gray hatching around the uptake zone is the region of dense cellular labeling. Dashed line indicates the white matter/layer 6 boundary. The injection site involves the subplate in a depth of 250ìm. (*B*) Side view of the monkey brain showing the region of prelunate gyrus which received injections in the present study. (*C*) Photomicrographs of injection sites in area V4 of E106, E123 and E140 fetuses (scale bars = 1 mm). WM, white matter injection; GM, gray matter injection. (*D*) Horizontal sections through the brain of an E140 fetus showing the location of the extrastriate and frontal areas where labeling is found in this study. Top left is dorsal and bottom right is ventral. Sections are numbered and representative levels indicated on the lateral view of the brain. Scale bar: 1 mm; abbreviations are given at end of paper.

infra- and supragranular labeled neurons (SLN%) and calculated separately for each projection zone (SLN% = number of labeled supragranular layer neurons/number of labeled supra + number of labeled infragranular layer neurons). SLN% falls off from a peak in the center of the projection zone to minimal values in the periphery (Barone *et al*., 1995, 2000; Batardière *et al*., 1998a). Fluctuating densities of supra- and infragranular layer neurons, coupled with the curvature of the cortical layers with respect to the plane of section, mean that stable values of SLN% require high frequency sampling of the entire projection zone.

Criteria for the Location of Cortical Areas

Multiple criteria were used to allocate labeled neurons to one of nine areas, including reference to gross morphological landmarks such as position in a particulars gyrus or sulcus (Barone *et al*., 2000); see Figure 2*D*. It was important to optimize the criteria used to distinguish different cortical areas, so as to be able to count neurons throughout a maximum extent of the projection zones in individual areas. Myelinization patterns and the laminar distribution of some histochemical staining in the fetus and neonate are immature and overall cannot therefore be used to identify cortical areas. Some architectonic limits were obtained using acetylcholinesterase histochemistry, which is strongly expressed in area V2 of fetuses and newborn (Barone *et al*., 1994).

One important criterion is the spatial distribution of labeling itself. Because the injection sites involved area V4 containing the representation of the central visual field, cortical areas which share borders where the far periphery of the visual field is represented show a discontinuous pattern of labeling. This gap in the labeling provides an important indication of the limits of the cortical area.

Area V2 is located in the posterior bank of the LS (Gattass *et al*., 1981), where it can be identified with cytochrome oxidase histochemistry in the adult (Tootell *et al*., 1983) and with acetylcholinesterase histochemistry in the fetus (Barone *et al*., 1994, 1996).

V3A is located in the anterior bank of the LS (Van Essen *et al*., 1986; Gattass *et al*., 1988; Felleman *et al*., 1997a). In most adult cases there is a gap between the labeling in areas V2 and V3A (Barone *et al*., 2000), while in fetuses this gap is less pronounced, but as in the adult there is a distinct increase in the density of labeling in the infragranular layers of area V3A. As in the adult, no labeling was found in area V3 on the anectant gyrus

(Barone *et al*., 2000). Because of the proximity of the injection sites to area V4t, it was difficult to separate the intrinsic labeling in area V4 from the extrinsic labeling in V4t. Consequently, we have not included V4t projections in the present analysis.

Area MT is located in the posterior bank of the STS and stretches from the fundus to about halfway up the sulcus (Van Essen *et al*., 1981; Maunsell and Van Essen, 1983; Ungerleider and Desimone, 1986). In the adult, there was a more or less pronounced gap between the labeling of area MT and labeling on the prelunate gyrus. In the fetus, labeling in MT was more continuous with area V4 and a posterior limit of MT was set in the sulcus so as to ensure that no V4t was included in our analysis of MT (Desimone and Ungerleider, 1986; Gattass *et al*., 1988).

Labeling was found in a visual motion area (FST) in the floor of the STS which is anterior and ventral to area MT (Desimone and Ungerleider, 1986; Ungerleider and Desimone, 1986; Boussaoud *et al*., 1990). The gap between labeling in area MT and FST was less apparent in the fetus than in the adult and the limit between these two areas was determined with reference to the fundus of the sulcus.

Labeling in the posterior and lateral bank of the IPS was isolated from labeling in other areas and corresponds to the lateral intra-parietal area (LIP) (Andersen *et al*., 1990; Blatt *et al*., 1990; Boussaoud *et al*., 1990; Baizer *et al*., 1991; Colby *et al*., 1996; Lewis and Van Essen, 2000a,b).

The major input to area V4 from higher order areas is from the visual areas in the temporal lobe. The temporal occipital area (TEO) is located on the temporal lobe between the IOS and the STS (Ungerleider and Desimone, 1986; Baizer *et al*., 1991; Boussaoud *et al*., 1991; Distler *et al*., 1993). In the adult, labeling was discontinuous between V4 and TEO, whereas in the fetus the limits between these two areas was determined by projecting the location of the gap in the adult on to charts of the cortical labeling in the fetus. Anterior and ventral to TEO in the inferior temporal cortex is the temporal area TE (Webster *et al*., 1991, 1994).

In the ventral region of the temporal lobe in the parahippocampal cortex are the cortical areas TF and TH, located medial to the rhinal fissure and posterior to the perirhinal cortex (Suzuki and Amaral, 1994). In the adult, SMI32 histochemistry and myelin stains can be used to delimit these temporal areas (Lewis and Van Essen, 2000a,b), but these markers are not expressed in the fetuses. Anteriorly and medially, labeling in TF/TH in the adult showed a gap with labeling in the ventral part of areas TE at the level of the rhinal fissure, while in the fetus labeling was sometimes continuous at this level. When this was the case, the position of the gap in the adult between ventral TE and TF/TH was projected on to charts of labeling in the fetus.

In the frontal cortex, labeled neurons were found systematically in the anterior bank of the AS which is known to house the frontal eye field – FEF or area 8 (Stanton *et al*., 1989; Schall *et al*., 1995)

Statistical Tests

A multinomial analysis of variance – ANOVA (Woodward *et al*., 1990) – was used to test the hypothesis that the SLN% is equal across visual areas. Infra- and supragranular layers were treated as within-subject factors in the analysis. By testing proportions, the problem of the variation in total number of cells was eliminated. The analysis did, however, incorporate the total numbers of labeled cells in the estimates of variance for each proportion, so that proportions based on small total numbers have less precision than those based on larger numbers. When a significant difference between areas was observed, the multinomial ANOVA allowed us to do planned comparisons and to identify the areas that violated the null hypothesis. To test the relationship between SLN% and the number of levels that separate two interconnected areas, derived from the adult hierarchy (Barone *et al*., 2000), we used the non-parametric Spearman rank correlation test.

Results

Injections in presumptive area V4 at all developmental stages lead to dense retrograde labeling throughout a large extent of extrastriate cortex (Figure 2). The criteria used for allocating neurons to individual areas are given in the Materials and Methods section and were central to a previous report (Barone *et al*., 2000). During development, retrogradely labeled neurons in the thalamus are confined to those regions of the lateral and inferior pulvinar which are known to project to area V4 in the adult (Baleydier and Morel, 1992; Adams *et al*., 2000).

Changes in Labeling Density Reflect Timetable of Innervation

So as to detect developmental increases in density of labeling resulting from innovation of the target, we have used a labeling index (*LI*) to monitor changes in the frequency of labeled neurons. *LI* is the percentage of labeled neurons with respect to the total population of neurons (Barone *et al*., 1996) and is not influenced by density changes due to developmental changes in cortical volume. Results for area V2, which is the major source of V4 afferents (Kennedy *et al*., 2000), are shown in Figure 3*A*. *LI* values show that at E106 only few cells have contacted their target (*LI* < 0.5%). Innervation proceeds steadily up to E129, when peak *LI* values are obtained (*LI*5%) before descending to adult-like values in the first postnatal month. This result suggests that the onset of cortical pathway formation is at E106, because this injection returned maximum levels of subcortical labeling coupled with only weak cortical labeling.

Influence of Injection of Subplate on Density of Labeling

The depth of the injection influences neuron density. This is illustrated in Figure 1 of the Supplementary Material where age-matched plots of retrogradely labeled cells in single sections of area V2 show higher densities of labeled cells in cases where the injection encroaches on the subplate (SP). A quantitative analysis of the effect of the injection extending into the SP at different ages is shown in Figure 3*C*. This shows that the involvement of the SP increases densities maximally at E123 and that the SP effect has largely disappeared by birth. This result shows that at early stages cortical axons are waiting in the SP.

Quantitative Analysis of Laminar Distributions

As described in the Materials and Methods section, quantification of SLN% within individual areas necessitates extensive sampling of projection zones (Barone *et al*., 1995, 2000; Batardière *et al*., 1998a). High-power plots of neuron location are made throughout the maximum extent of labeling at regular intervals (see Supplementary Material). In the adult these charts provide an overview of changes in neuronal labeling density in different cortical areas. Such qualitative comparisons of adult and fetal labeling also give an indication of the developmental reduction of labeled supragranular layer neurons. Counts of numbers of neurons per section in each area make it possible to construct neuron density profiles of the projection zone in each area (Fig. 4) following each injection. This ensures that counts include peak values of the projection zone. Figure 4 illustrates the impossibility of using only two or three sections to estimate SLN%. For example, in the adult the profile for MT (Fig. 4*C*) returns global values of 55%, whereas individual sections from this injection return values ranging from 6 to 93%. The estimation of SLN% is computed directly by summing the total number of labeled neurons in the density profile for each area and for each injection.

Developmental Remodeling

The density of labeled neurons at E106 is very low and increases up to E123 (Fig. 3*B*). This and the fact that distant areas have low numbers of labeled neurons, or in the case of FEF and TE none at all, further supports that cortico-cortical axons begin to innervate their targets some time around E106.

In a first instance we shall consider FB projections obtained at the later fetal stages investigated (i.e. E112, E123, E140). SLN% in

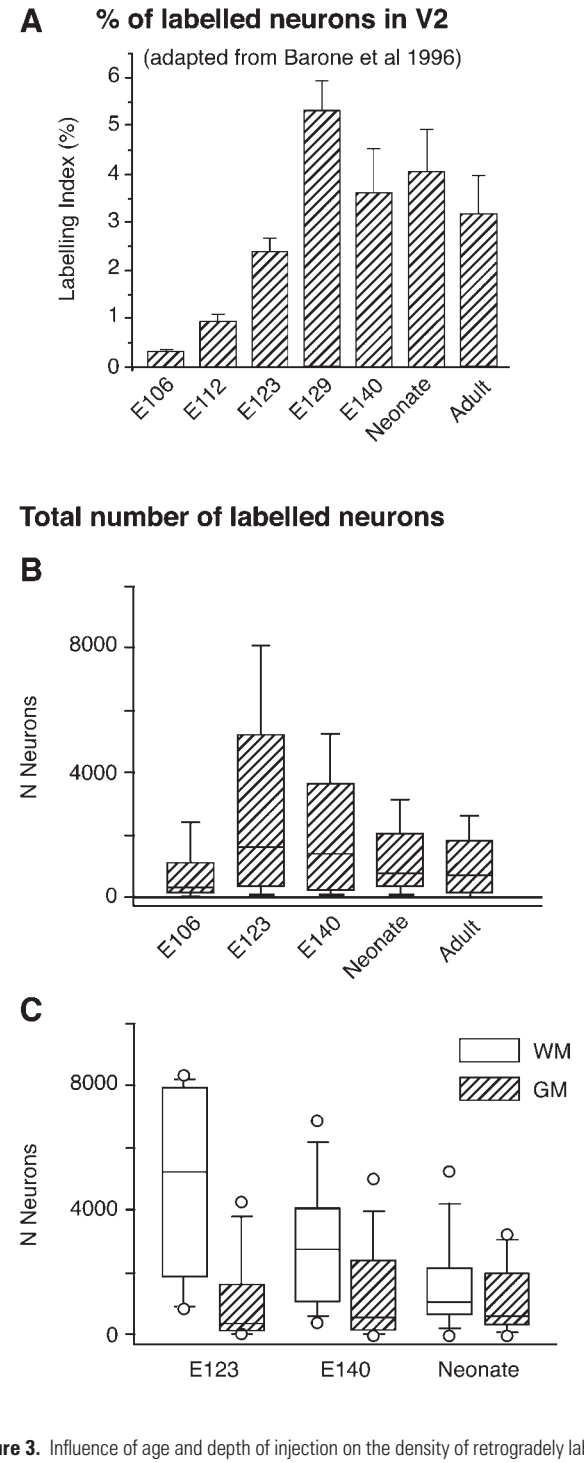

Figure 3. Influence of age and depth of injection on the density of retrogradely labeled cells. (*A*) Histogram of the proportion of labeled cells in area V2 (labeling index) with respect to the total number of unlabeled cells determined on Nissl stained sections [adapted from Barone *et al*. (Barone *et al*., 1996)]. The labeling index is low at E106, suggesting that this age corresponds to the beginning of the establishment of the V2 to V4 connection. The labeling index is maximum at E129 and decreases to lower values in the adult. (*B*) Box plots displaying the distribution of the total number of retrogradely labeled neurons observed in each area during the development. For comparisons between ages, the sampling frequencies were the same at all ages for each area. At E106, only a low number of cells were labeled, the density reaches a peak at E123 and decreases progressively to lower values in the adult. (*C*) Box plots displaying the distribution of the total number of neurons observed in each area in developmental cases where white matter and gray matter injections were simultaneously performed (see Table 1). In fetuses a WM injection leads to a much higher number of labeled cells compared to an injection restricted to the gray matter. No such effect was observed at birth. The injection sites of the corresponding fetal cases are shown in Figure 2.

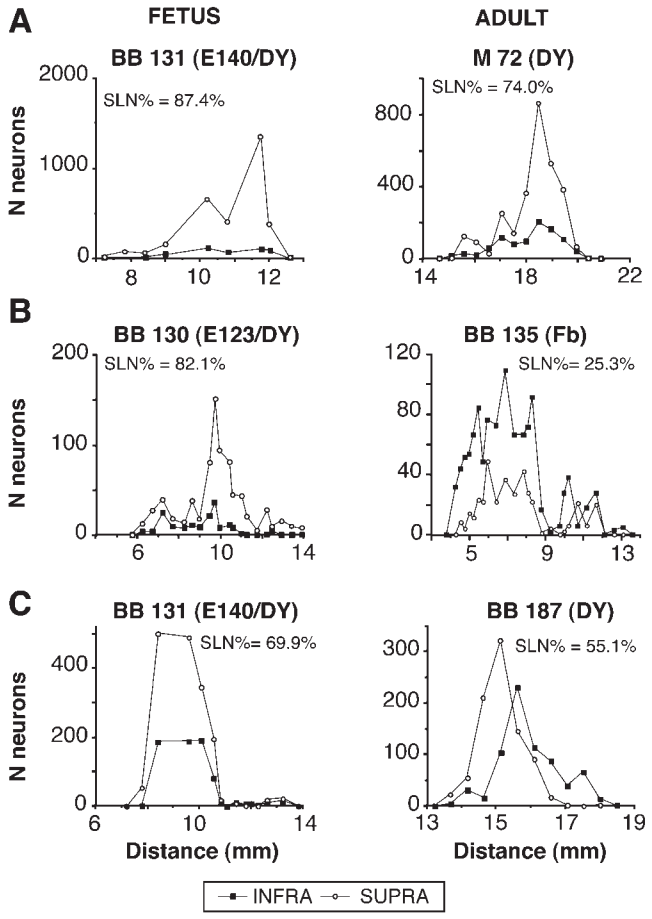

Figure 4. Density profiles of the infragranular layer (black squares) and supragranular layer neurons (open circles) in areas V3A (*A*), LIP (*B*) and MT (*C*) in fetuses (left) and adults (right). This represents the distribution of the number of labelled neurons across the area. For each case, global values of SLN% are provided at each age. All cases of density profiles derived from an injection restricted to the gray matter.

higher-order areas (LIP, FST, TEO, TE, TH/TF) tends to fall into one of three groups: high (late fetal ages), medium (neonates) and low (adults and juveniles animals) (Fig. 5*D*,*E* and Table 2). The four injections in both of the 2 month old animals give results which are statistically indistinguishable from the adults (multinomial ANOVA, $\chi^2 = 4.75$, $P = 0.09$, n.s.) and these values therefore are pooled. A statistical analysis revealed that values in late fetuses differ significantly from those observed in neonates ($\chi^2 = 772.3$, $P < 0.001$). Furthermore, except for TE and TH/TF, all the percentages returned by the neonate injections are intermediate between late fetal stages and adult values ($\chi^2 = 51.14$, $P < 0.001$), showing that cortical connectivity is not fully mature at birth.

In the FF projections, SLN% in area V2 remains constant at different developmental stages (*post hoc* comparison, fetus versus adult: $\chi^2 = 0.09$, $P > 0.5$; Fig. 5*A*). This contrasts with a weak (20%) but significant SLN% reduction in area V3A ($\chi^2 = 24.23$, $P < 0.001$). The lateral connections from area MT in the E112–140 fetuses (Fig. 5*B*) are concentrated in the supragranular layers (SLN% = 66%), which contrasts with the adult where these connections are more evenly distributed in both layers (SLN% = 47%) so that the development reduction of SLN% is 28%. The FB projections from all areas in both dorsal and ventral streams show important reductions in SLN% (Fig. 5*D*,*E*).

Table 2

SLN% values following V4 injections at different developmental ages. For all areas where labeling was observed, the SLN%, the number of neurons (N Nr) and the number of sections sampled (N Sct) are indicated

Case		Age	V1			V2			V3A			MT			FST		
			SLN%	N Nr	N Sct	SLN%	N Nr	N Sct	SLN%	N Nr	N Sct	SLN%	N Nr	N Sct	SLN%	N Nr	N Sct
BB 115 Fb	[b]	E 106	100.00	1	15	90.92	2402	15	74.98	1471	7	53.92	5758	22	30.18	497	14
BB 109 Fb[a]	[b]	E 112										64.76	12 146	12	61.15	3561	10
BB 130 Fb*	[b]	E 123	84.48	464	14	91.51	12 635	12	67.02	8119	6	62.67	6052	10	46.59	2127	7
BB130 DY	[b]	E 123	81.82	11	14	96.93	5089	12	79.17	3077	6	78.30	1498	9	46.88	320	7
BB 131 Fb*	[b]	E 140	97.99	349	8	94.66	11 547	13	64.65	4458	9	53.70	6722	16	46.60	1854	12
BB 131 DY	[b]	E 140		0	8	97.12	3684	11	87.36	3551	8	69.90	2389	15	70.31	128	13
BB 127 Fb*	[b]	PND 6		0	11	95.16	4462	11	68.83	4290	11	47.25	2034	15	34.34	964	11
BB127 DY	[b]	PND 6		0	10	98.36	5676	10	72.87	2702	8	64.89	2569	10	34.65	490	11
BB187 Fb	[c]	PND 59	100.00	46	14	94.23	3724	35	58.37	1201	21	46.67	1395	12	4.95	222	19
BB187 DY	[c]	PND 59	100.00	10	14	98.87	4591	33	67.21	2458	21	55.10	1579	12	2.08	144	19
BB119 Fb	[b]	PND 61	100.00	9	13	88.77	3162	21	51.73	2111	15	47.12	832	19	44.76	286	11
BB119 DY	[b,c]	PND 61	100.00	2	13	84.62	3362	21	47.03	1916	15	43.37	618	19	9.46	74	11
BB135 Fb	[c]	PNM 13	100.00	1	14	96.46	3620	14	67.84	768	6	25.65	5610	19	14.80	304	12
M72 Fb	[c]	Adlt	100.00	7	30	94.09	8454	30	52.05	3218	13	57.37	1283	12	12.86	933	26
M72 DY	[c]	Adlt		0	30	96.71	5136	30	74.02	3603	13	54.77	953	10	8.42	463	24

Case		Age	LIP			TEO			TE			TH-TF			FEF		
			SLN%	N Nr	N Sct	SLN%	N Nr	N Sct	SLN%	N Nr	N Sct	SLN%	N Nr	N Sct	SLN%	N Nr	N Sct
BB 115 Fb	[b]	E 106	43.73	359	28	13.07	528	17				11.21	437	14		0	20
BB 109 Fb*	[b]	E 112	52.94	918	9	59.41	9800	10	43.20	1213	9				65.33	548	15
BB 130 Fb*	[b]	E 123	72.13	6404	21	69.04	4955	10	59.75	5354	10				74.85	862	29
BB130 DY	[b]	E 123	82.11	928	21	76.54	810	10	70.87	103	10				73.20	153	27
BB 131 Fb*	[b]	E 140	44.14	1015	19	52.94	4080	9	29.69	3604	12	11.38	1046	11	73.57	908	21
BB 131 DY	[b]	E 140	54.84	155	12	71.67	1645	8	38.75	929	12	0.00	31	10	60.66	211	17
BB 127 Fb*	[b]	PND 6	38.77	962	16	46.90	8251	14	8.08	4339	13	0.41	1206	8	67.55	604	19
BB127 DY	[b]	PND 6	39.70	1010	16	51.95	2722	10	38.31	804	11	1.19	335	8	57.89	133	16
BB187 Fb	[c]	PND 59	22.22	99	15	43.27	2281	13	35.94	2485	17	0.00	600	11	71.79	39	15
BB187 DY	[c]	PND 59	22.55	102	15	30.65	1589	13	32.16	1480	17	0.00	259	11	95.65	23	15
BB119 Fb	[b]	PND 61	59.76	410	21	57.06	3214	19	31.54	1379	13	4.77	818	6	69.62	339	23
BB119 DY	[b c]	PND 61	25.13	593	21	39.52	2735	19	14.04	413	13	0.00	95	6	53.33	105	23
BB135 Fb	[c]	PNM 13	25.26	1461	26	47.06	5861	16	8.11	2477	16	0.59	850	13	68.14	521	17
M72 Fb	[c]	Adlt	23.56	191	14	36.45	2524	9	30.45	3327	14	0.38	788	12	76.34	93	11
M72 DY	[c]	Adlt	9.90	202	14	24.44	753	9	28.00	1193	14	0.00	415	12	73.02	63	11

[a]Injections that involve the subplate.

[b]Cases used in previous publication (Barone *et al.*, 1996).

[c]Cases used in previous publication (Barone *et al.*, 2000).

Conventions as in Table 1.

In the adult and fetus the FEF V4 pathway show stable values (70 versus 73%, $\chi^2 = 0.057$, $P > 0.05$).

Because we have results from only one animal per age group, we cannot evaluate variability in SLN% at fetal ages. However, in the adult a statistical analysis did not reveal significant differences in SLN% across subjects (see above, $\chi^2 = 4.75$, $P = 0.09$) or because of the type of dyes used when a double injection was performed in the same animal (Fb versus DY, all cases $P > 0.05$). Furthermore, when individual SLN% are plotted against age (Fig. 5*F*), the developmental curves follow a regular monotonic decrease from E123 to juvenile–adult values. Taken together, these observations suggest that at each fetal age and in the adult, single-dye injection provides stable SLN%.

Cellular Mechanisms and Timetable of Developmental Remodeling

The cortical and subcortical patterns of labeling at E106 suggest that the great majority of cortical axons have not yet reached their targets at this age. In all areas (except in TH/TF) SLN% of the E106 fetus are lower than those obtained in older fetuses (Fig. 5). The increase in SLN% between E106 and E123 occurs over a time period when there is an important increase in overall numbers of projecting neurons (Fig. 3*B*). This suggests that it is the consequence of an increase in the number of supragranular rather than a reduction in the numbers of labeled infragranular layer neurons. Hence, it would seem that although development is characterized by excess numbers of SLN, the very early axons to arrive in the cortex at E106 are mostly from infragranular layers (Coogan and Burkhalter, 1988).

At late developmental stages (E123, E140, neonate) a DY and an Fb injection has been made side-by-side in area V4 (see Fig. 2). In each case, the Fb injection involves the underlying SP whereas the DY injection is entirely restricted to the cortical gray matter (GM injections). SP injections label higher numbers of neurons compared to GM injections (Fig. 3*C*). However, GM injections lead to higher SLN% in all areas (V3A, MT, TEO, TE and LIP) compared to SP injections at the same age (Fig. 6*A*). The most pronounced increase of SLN% following GM injection is observed at E140. Overall, GM injections give a mean increase in SLN% of ~13% compared to SP injections. These results mean that the SP injections lead to proportionally more axons from infragranular layer neurons capturing and retrogradely transporting the dye than do GM injections. We can deduce, therefore, that from E123 to birth there is a delay in the ingrowth of the infragranular axons into the cortical gray matter of their targets. Note that the developmental SLN% reduction is observed

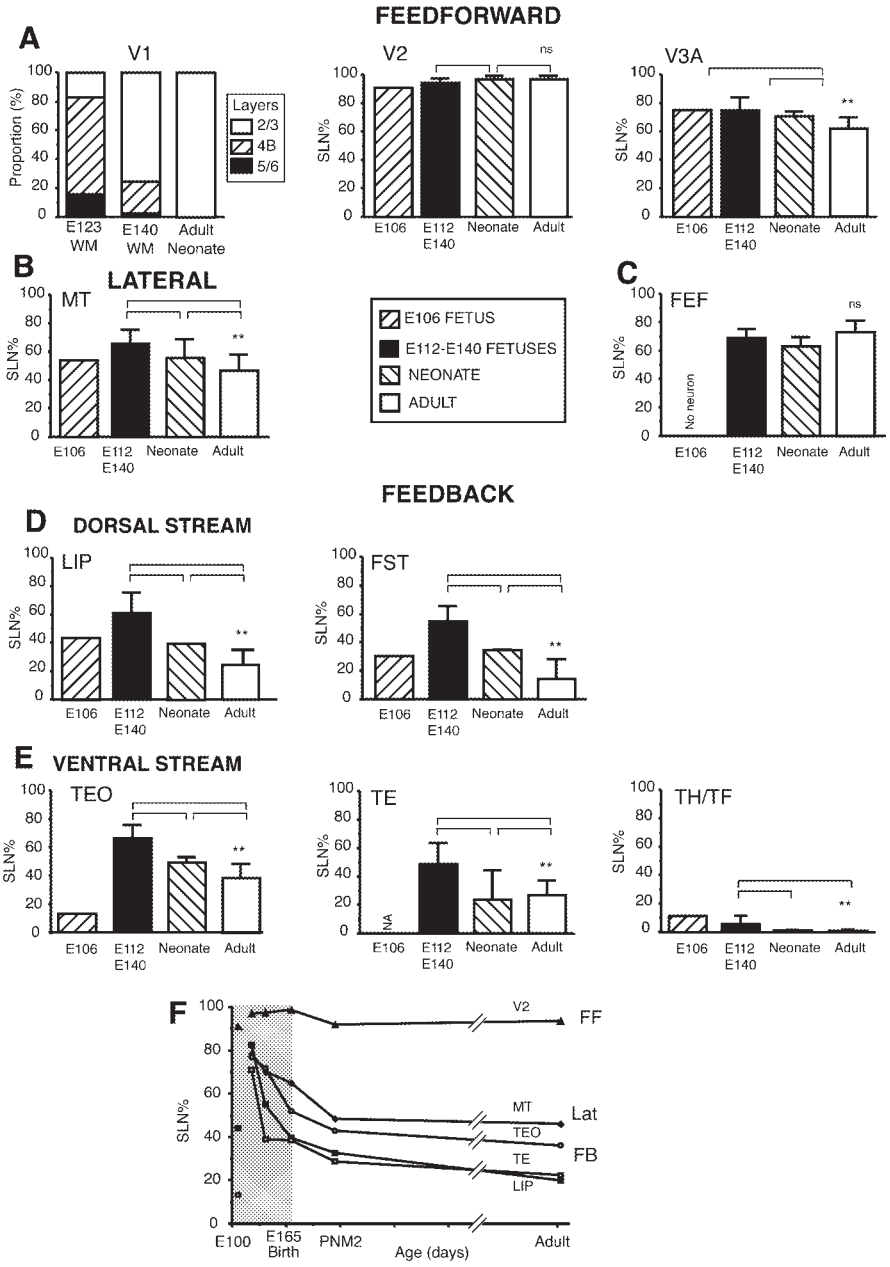

Figure 5. Laminar remodeling of afferent connections to V4. (*A–E*) Histograms of the mean percentages of labeled supragranular layer neurons (SLN%) in individual cortical areas in fetuses, neonates and adults. Because of the presence of labeling in layer 4B, data in area V1 are expressed differently, the histogram corresponds to the proportion of labeled cells in three laminar compartments (layers 2/3, layer 4B and layers 5/6). Bars link pairs of ages for which SLN% were statistically different. Levels of statistical significance are indicated between E112–E140 fetuses and adults (n.s., non significant; $^{**}P < 0.01$). (*F*) Developmental evolution of SLN% with age. Data are shown for SLN% values obtained following a gray matter injection for five representative areas. For lateral (MT) and feedback (TEO, TE and LIP) projections there is a continuous decrease in SLN% during prenatal ages to reach adult-like values 2 months after birth. No significant variations in SLN% were observed in feedforward projection (V2).

when considering both SP and GM separately (data not shown). Hence, the depth of injection does not influence our results when data from all injections are pooled.

Side-by-side injections of DY and Fb lead to two populations of single-labeled neurons with a variable degree of spatial overlap, depending on the distance separating the two injection sites. Neurons which project to both injection sites capture both dyes (i.e. are double-labeled) and are located in the overlap zone of the two populations of single-labeled neurons (Kennedy and Bullier, 1985; Barone *et al.*, 1995). In the adult FB and lateral pathways, maximum numbers of double-labeled neurons are located in the infragranular layers (Fig. 6*B–F*), which reflects the fact that the spatial extent of the projection zone in the adult is greater in the infragranular layers than it is in the supragranular layers. At fetal stages the majority of double-labeled neurons are located in the supragranular layers, suggesting that at these stages the projection zone in the supragranular layers extends further than those in the infragranular layers (Fig. 4). This finding suggests that supragranular layer neurons undergo a developmental reduction of their divergence (i.e. a reduction of the extent of the target area contacted by individual neurons).

Remodeling and Hierarchical Organization

In the adult we have shown that a pathway connecting two areas

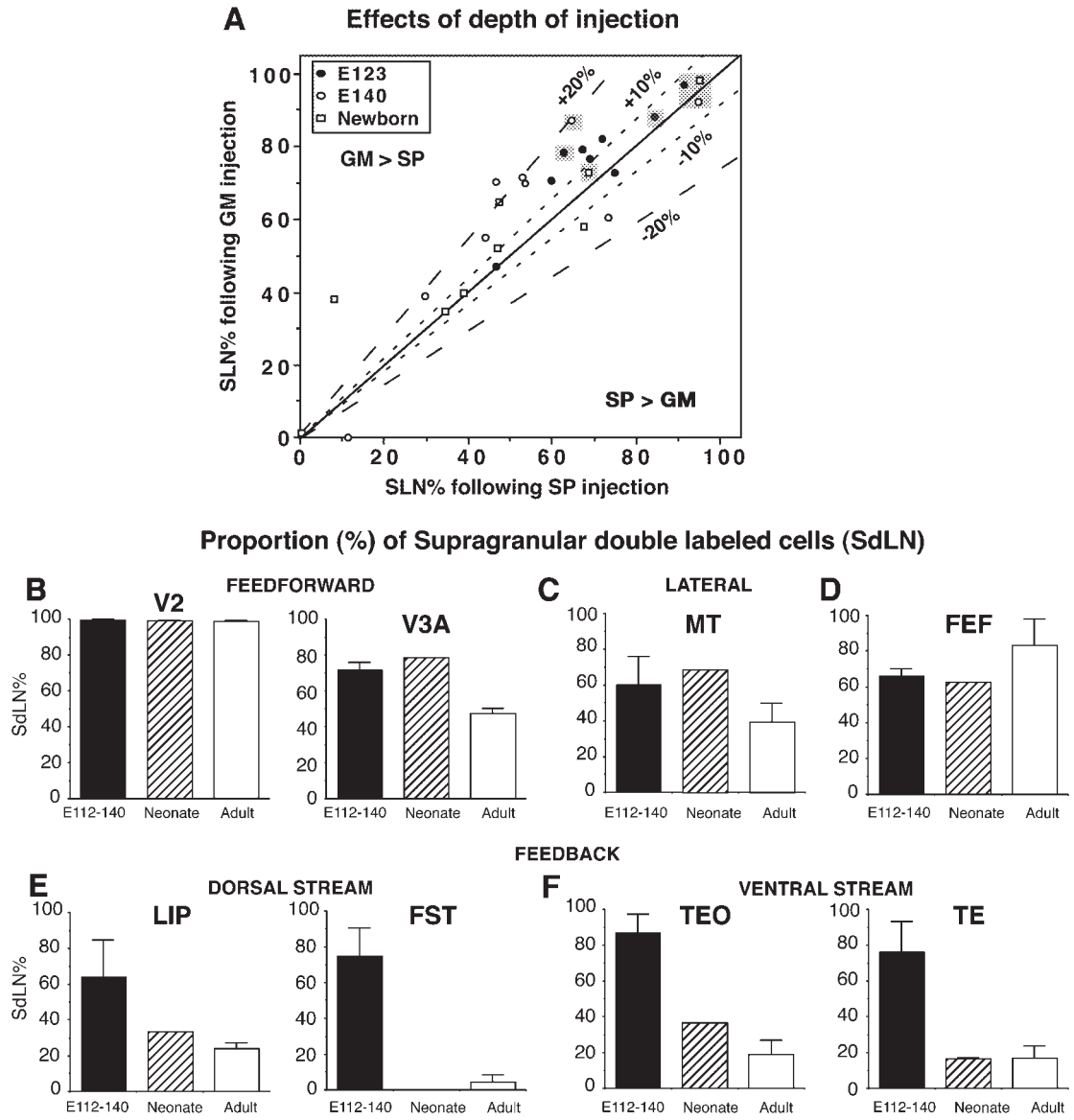

Figure 6. Cellular mechanisms of remodeling. (*A*) Scattergram of SLN% values obtained from each of the pairs of injections in a single animal following a subplate (SP) and gray matter (GM) injection. In 22/26 (85%) cases, a GM injection produces higher SLN% values than a SP injection. Dashed lines represent ±10% or ±20% deviation from the equality (plain line). Cases corresponding to FF pathways are up-lightened in gray. (*B–F*) Histograms of the percentage of double-labeled neurons located in the supragranular layers (SdLN%) of fetuses, neonates and adults. Conventions as in Figure 5.

is characterized by its SLN% and reflects the number of hierarchical levels that separate the two interconnected areas (Barone *et al.*, 2000); for details of calculation see the legends of Figures 1 and 7. In adult FB pathways, increasing the number of levels between interconnected areas decreases SLN%. In adult FF pathways it is the inverse, so that increasing the number of levels between interconnected areas increases the SLN%. This we refer to as a 'distance rule'. Inspection of the laminar organization of the pooled projections in fetuses (E112–E140, Fig. 7*A*) suggests that the same distance rule applies during development. As in the adult, SLN% in fetuses are specific for each projection (χ^2 = 24 523; $P < 0.001$). However, in fetuses differences between SLN% are not as marked and the overall increase of the SLN% means that there is a reduced dynamic range.

In the adult, SLN% can be used to rank areas on distinct hierarchical levels – see Figure 7*B* (Barone *et al.*, 2000). A similar statistical approach was applied to the pooled fetal SLN% values. The paired comparisons of SLN% from each area reveal that 42 out of 45 are significantly different (Table 3). Furthermore, this analysis shows that 45 pairwise comparisons in the fetus reveal 87% homology with the same analysis performed in the adult (39/45 comparisons, Table 3). As in the adult, SLN% in the fetus put V2, V3A as well as ventral areas TEO, TE and TH/TF on successive levels. Furthermore, as in the adult, fetal SLN% values for the FEF place this area on a low hierarchical level, equivalent to that of V3A ($\chi^2 = 0.61$, $P = 0.43$, n.s.). Similarly, as in the adult, fetal SLN% values place MT and TEO on the same level ($\chi^2 = 0.76$, $P = 0.38$, n.s.) and put FST and LIP on separate levels ($\chi^2 = 79.29$, $P < 0.001$). In the fetus there is a strong and significant correlation (Spearman, = –0.83, $P = 0.01$, Fig. 7*B*) between SLN% and the hierarchical distance using the hierarchical model of the adult visual system proposed by Barone *et*

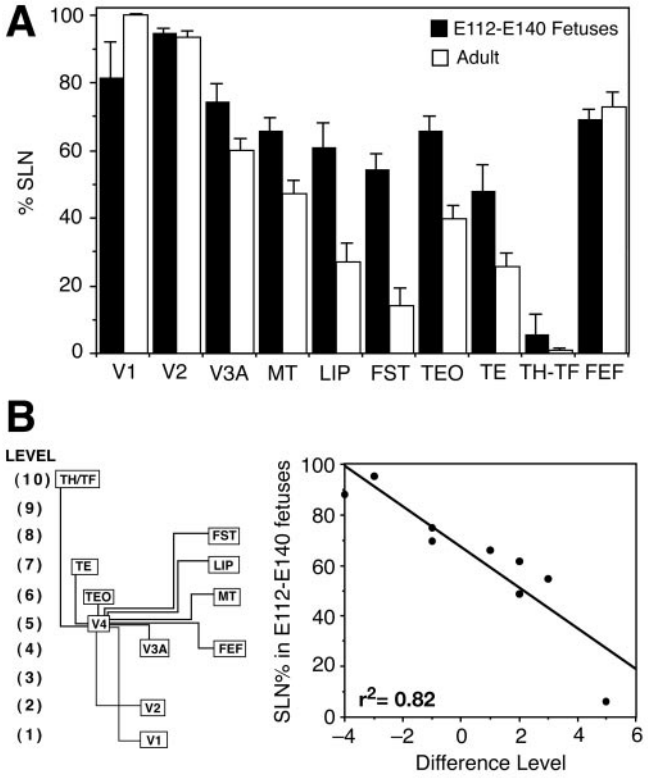

Figure 7. Remodeling and hierarchical organization. (*A*) Summary of SLN% (see Fig. 5) observed in all areas projecting to V4 in E112–E140 fetuses (gray bars) and the adult (white bars). These histograms show the continuum of SLN% values observed across areas and reveal that in fetuses and in the adult, SLN% are characteristic of each individual projection. (*B*) Left-hand panel: position of each areas that project to V4 according to Barone *et al.*'s adult hierarchical organization of the visual system (Barone *et al.*, 2000). Right-hand panel: relationship between SLN% and the hierarchical distance (difference level) that separates V4 from its interconnected areas in fetuses. For each pathway we have calculated the number of hierarchical steps separating a projecting area from area V4, i.e. difference level = (level of the projecting area) – (level of area V4). Thus in FF pathways to V4, difference levels are negative while for FB pathways difference levels are positive.

Table 3

Statistical comparisons. Multinomial analysis of variance was used to test differences in SLN% across visual areas in adult (upper, from Barone *et al.*, 2000) and fetuses (lower). c^2 and *P*-values are provided. For the analysis in fetuses, areas were treated as between group factors

Adult DY: $\chi^2 = 14\,073$; $P < 0.001$ FB: $\chi^2 = 13\,185$; $P < 0.001$

	V1	V2	V3A	MT	FST	LIP	TEO	TE	TH/TF	FEF
V1		<	<	<	<	<	<	<	<	<
V2	NA		<	<	<	<	<	<	<	<
V3A	NA	**		<	<	<	<	<	<	=
MT	NA	**	**		<	<	=	<	<	>
FST	NA	**	**	**		>	>	>	<	>
LIP	NA	**	**	**	***		>	=	<	>
TEO	NA	**	**	*/NS	**	**		<	<	>
TE	NA	**	**	*	**	*/NS	**		<	>
TH/TF	NA	**	**	**	**	**	**	**		>
FEF	NA	**	*/NS	**	**	**	**	**	**	

Fetus $\chi^2 = 7712$; $P < 0.001$

	V1	V2	V3A	MT	FST	LIP	TEO	TE	TH/TF	FEF
V1		>	<	<	<	<	<	<	<	<
V2	*		<	<	<	<	<	<	<	<
V3A	***	***		<	<	<	<	<	<	=
MT	***	***	***		<	>	=	<	<	>
FST	***	***	***	***		>	>	<	<	>
LIP	***	***	***	***	***		<	<	<	=
TEO	***	***	***	NS	***	***		<	<	>
TE	***	***	***	**	***	***	***		<	>
TH/TF	***	***	***	***	***	***	***	***		>
FEF	***	***	NS	***	***	NS	***	***	***	

Statistical levels of significance are indicated for the planned comparisons of SLN% between pairs of area (NS, non significant; *$P < 0.01$; **$P < 0.001$). These comparisons are used to rank pairs of areas (higher, >; lower, <; same level, =). Boxes highlighted in gray correspond to cases where the statistical comparisons between areas in the fetus differed to that obtained in the adult (6/45 cases).

al. (Barone *et al*., 2000) and a somewhat lower correlation (Spearman, ρ = –0.78, $P = 0.01$; $r^2 = 0.71$ versus 0.82). using the hierarchical scheme proposed by Felleman and Van Essen (Felleman and Van Essen, 1991). The fact that the fetal values show a close correlation with the adult hierarchy strengthens the idea that the hierarchical relationships remain constant during development, despite the overall higher SLN% values in the immature cortex.

Values of SLN% differ significantly between E123 and E140 (multinomial ANOVA, $\chi^2 = 217.5$, $P < 0.001$) and from E140 to birth ($\chi^2 = 269.2$, $P < 0.001$). Using SLN% at individual ages (123, 140, newborn), we obtain adult-like sequences in ventral (TEO > TE > TH) and dorsal (FEF > MT > FST) streams. The progressive emergence of the adult organization during development can be assessed by analyzing the correlation of hierarchical rank and SLN% at different ages (Fig. 8*B*). At all stages (E106, E123, E140 and neonate), there is a significant correlation between the SLN% and hierarchical rank (Spearman, $P < 0.05$) except in the case of the gray matter injection at E123 (Spearman, ρ = –1.67, $P = 0.09$). The fact that the GM injection at E123 gives a weaker correlation than the SP injection at the same age is because of the high number of axons from supragranular layers that have penetrated the target at this age. The SP injection returns a lower SLN% because it recruits the waiting infragranular layer neurons.

As seen in Figure 8*D*, there is a progressive increase in the steepness of the correlation slope from E123 to birth, when adult-like values are observed. Similarly, the correlation factor (r^2) increases with development and by birth returns values similar to those obtained in the adult (Fig. 8*C*). Overall, this analysis shows that hierarchical ranking of visual cortical areas is established in the fetus and, further, that it is only marginally influenced by extending the injection into the SP.

Although an adult-like sequence is present in fetal stages, SLN% are overall significantly higher in the fetus compared to the adult. SLN% reduction influences differentially each FB pathway to area V4. For example, between E123 and adult (Fig. 8*E*), in the dorsal pathway, the reduction in SLN% is progressively higher going from V3A (–20%), MT (–33%), LIP (–65%) and FST (–71%). A similar increase in reduction is observed in the ventral pathway going from TEO to TE. In Figure 8*F*, the decrease in SLN% for individual projections to V4 is plotted against the number of hierarchical levels, i.e. hierarchical distance (Barone *et al*., 2000), separating each area from area V4. In fetuses, the amplitude of reduction (E123 adult, E140 adult) is tightly related to the hierarchical distance (both cases, Spearman, $P < 0.01$). From birth to adulthood, the remodeling is weaker than in fetuses (see Fig. 5) and is not correlated with the hierarchical distance to V4 (Spearman, ρ = –0.27, $P > 0.05$).

Altogether, although global SLN% is higher in the fetus compared to the adult, the hierarchical ranks are clearly established in the immature cortex. Hence, differences of SLN% are sharp enough to maintain a distance rule (and therefore hierarchical levels) and thus the relative relations between areas

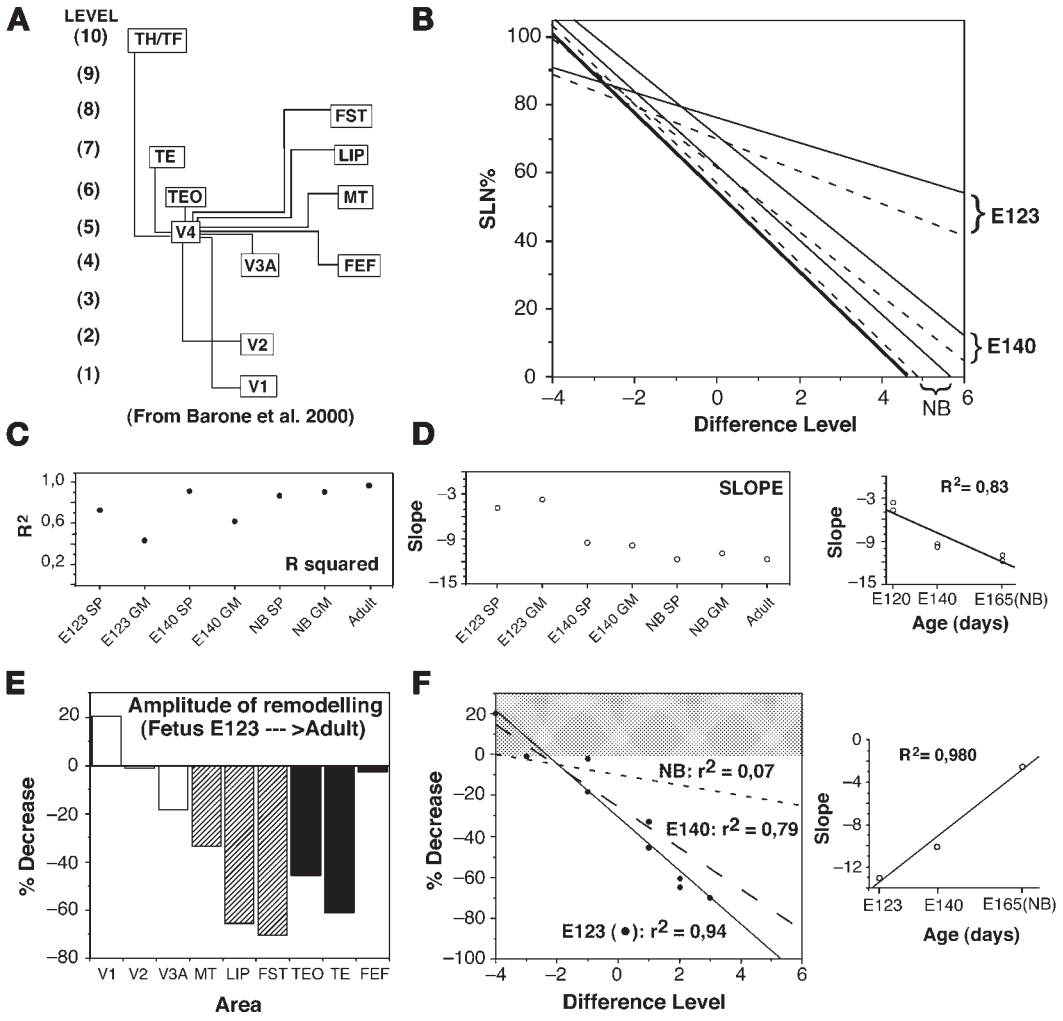

Figure 8. Early establishment of hierarchical organization. (*A*) Left-hand panel: position of each areas that project to V4 according to Barone *et al.*'s adult hierarchical organization of the visual system (2000). (*B*) Co-relationship for individual injections at all developmental stages, of SLN% with the number of hierarchical levels that separate V4 from its afferent areas. Dashed lines are cases where the injection involved the subplate. The bold line correspond to the correlation obtained from the adult values (Barone *et al.*, 2000). (*C*) Correlation coefficient (r^2) calculated from the individual correlograms shown in (*A*). (*D*) Left-hand panel shows the slope values calculated for the individual correlograms. The right-panel shows the progressive increase in the values of the slope during the development. Note that results obtained at E112 are not included because of incomplete data. (*E*) Amplitude of SLN% reduction observed between fetal (E123) and adult stages in each area projecting to V4. (*F*) Relationship between the amplitude of SLN% reduction with respect to the adult and the distance (difference level) that separates V4 from its interconnected areas in fetuses (E123 and E140) and the neonate (NB). For clarity, only individual data points from E123 are shown. The right-hand panel shows the progressive decrease in the values of the slope during development. Conventions as in Figure 7.

are as in the adult. The adult SLN% is, however, established progressively through a prolonged developmental period that lasts until the first month after birth.

Discussion

Technical Considerations

Because immunohistochemistry and myelin stains can not be used in the fetus to define cortical areas, a major difficulty in a developmental study such as this is the correct allocation of neurons to individual cortical areas. In the present study, we found that projections from individual areas originate from well-defined projection zones showing peak levels of labeling (see Fig. 4). This means that immature cortico-cortical projections do not form a uniform distribution, but instead link spatially defined regions of the cortex which correspond to future cortical areas. Although the immature material did not show clearly defined gaps between labeled regions (see Materials and Methods), it is unlikely that imprecision on the exact position of areal borders significantly influences the present results, given that peak levels were centered in the presumptive cortical areas. Hence, while uncertainty regarding the exact location of areal borders might introduce a small degree of error, in the present findings this does not influence the major result, which is that the number of labeled neurons peaks in presumptive cortical areas and that SLN% are characteristic for each area.

Primate developmental studies such as this invariably suffer from using small numbers of animals at each developmental stage. This means that the variable which is to be measured needs to be highly reliable. This is, in fact, the case. In the adult we have shown that, correctly assessed, SLN% values across individuals are constant and are extremely robust indicators of hierarchical rank (Barone *et al.*, 2000).

Time Course of Remodeling

We are confident that we have encompassed the developmental period during which cortical connections undergo reorgan-

ization. Our first injection at E106 showed that few connections from afferent cortical areas had been made with the cortical gray matter of area V4, despite the fact that injections in the SP at this age reveal numerous projections (Coogan and Van Essen, 1996). The present study shows that the laminar distribution for projections to area V4 matures according to a similar time course as those back-projecting to area V1, where the adult configuration is achieved 1–2 months after birth (Barone *et al*., 1995).

Comparison with other Species

In the kitten, the laminar distribution of FB projections to area 17 is uniform across individual extrastriate areas and the selective reduction of the SLN% generates the laminar distribution characteristic of each area (Batardière *et al*., 1998a). This contrasts with the primate, where FB projections to area V1 show a rudimentary areal specificity right at the start of cortico-cortical pathway formation, as has been shown in this report and elsewhere (Barone *et al*., 1995). The present results show that those pathways which project to area V4 and which show a developmental remodeling (i.e. from areas V3A, MT, FST, LIP, TEO, TE, TH/TF) are also specified from the onset of pathway formation and therefore exhibit characteristic SLN% values during early stages of development prior to developmental remodeling of the pathway. In this way, in the primate the reduction of SLN% serves to sharpen an early formed pattern.

Cellular Mechanisms Underlying Developmental Changes in the Laminar Distribution

The developmental reduction of SLN% in FB projections to area V1 has been shown to be accompanied by a larger decrease in the convergence values of supragranular projection neurons compared to infragranular projection neurons (Barone *et al*., 1995, 1998; Batardière *et al*., 1998a). In the present study, the switch of double-labeled neurons from a supragranular location in the fetus to an infragranular layer location in the adult suggests that the remodeling of the laminar distribution for projections to area V4 is also due, at least in part, to a reduction of the convergence values of cortico-cortical connections (Kennedy *et al*., 1994; Price *et al*., 1994).

Which cortical layer first forms a projection with its cortical target? This question is important because the process of path-finding and target recognition might be expected to be the prerogative of these first-formed connections. The present results, showing that at the very earliest age (E106) the few cortical connections from higher-order areas stem from infragranular layers, suggests that the earliest born neurons might be the first to send an axon to their appropriate cortical target early in development (Coogan and Burkhalter, 1988). Such a developmental strategy would make sense because when the layer 6 neurons have just completed their migration to the cortex at ~E70, the distances separating cortical areas are considerably shorter than at E100 when upper layer neurons begin to form connections. The present results show that after E106, injections involving the SP lead to an appreciably lower SLN% than do injections restricted to the cortical gray matter. This suggests that a fraction of axons from infragranular layer neurons have not yet invaded the cortical gray matter in the immature brain between E120 and birth. Hence, it would be reasonable to conclude that the axons of infragranular neurons are the first to contact the target where one subpopulation remains in the SP while some axons penetrate the GM. Subsequently, axons from the supragranular layers penetrate the cortex in large excess. At this late stage the infragranular axons continue to form an appreciable number of transient connections with the SP. In this way, formation of cortical connections involves two sets of transient connections: the first from the infragranular neurons to the SP of the target and the second from the supragranular neurons with the GM of the target area. Elimination of these transient connections follows different timetables. Elimination to the SP is complete by birth and to the GM 1 month later. Thus, the late invasion of the GM by infragranular axons along with the reduction of convergence of supragranular layer axons, contributes to establishing the mature SLN%.

Conclusion

The development of the cortical connectivity of area V4 illustrates a highly dichotomous strategy in the formation of FF and FB pathways. The development of the FF pathway from area V2 to area V4 has been shown to be complete early in prenatal life, to depend largely on directed growth and target recognition mechanisms and not to involve the large-scale elimination of inappropriate axons (Barone *et al*., 1996). Supragranular layer neurons constitute the major component of the FF pathway and their axons accurately target their final destination early in development. This contrasts with the prolonged remodeling of the FB projections, where selection leads to a massive pruning of early formed connections but where late progressive factors may also play a role as has been demonstrated in this study and elsewhere (Rodman, 1994; Barone *et al*., 1995).

In the adult, SLN% values are highly specific for individual cortical areas (Barone *et al*., 2000). Because the exact SLN% is related to the hierarchical distance separating cortical areas, it is expected in turn to relate to the physiological role of FF and FB pathways which are beginning to be understood from both ultrastructural and physiological investigations (Ishai and Sagi, 1995; Miyashita, 1995; Vanduffel *et al*., 1997; Anderson *et al*., 1998; Gonchar and Burkhalter, 1999; Lamme and Roelfsema, 2000). Throughout development we observed that the relative hierarchical organization of the visual system is similar to that in the adult.

The early prenatal specification of FF connections could provide the neurophysiological substrate for the steady increase of visual capacities observed in infant monkeys during the first postnatal months (Blakemore and Vital-Durand, 1981; Boothe *et al*., 1985; Rodman *et al*., 1993; Rodman, 1994; Distler *et al*., 1999). However, the adult laminar organization of FB pathways is not present before the second postnatal month. This prolonged development of FB cortical connections might be of particular importance in primates, as we also detected this phenomenon in the somatosensory system (Batardière *et al*., 1998b) and one would predict that this could be further extended in humans (Burkhalter, 1993; Kennedy and Dehay, 1997; Kennedy *et al*., 1997). Given the evidence of the involvement of FB projections in figure ground discrimination (Zipser *et al*., 1996; Hupé *et al*., 1998), it is interesting to note that this psychophysical response emerges at the end of the first year of life and only becomes adult-like at around 8–13 years of age in human (Sireteanu and Rieth, 1992). The searching question that remains is why would FB pathways in the visually experienced infant include 28–84% additional supragranular layer projection neurons?

Supplementary Material

Supplementary material can be found at:
http://www.cercor.oupjournals.org

Abbreviations

Cortical Visual Areas

V1	visual area 1
V2	visual area 2
V3	visual area 3
V4	visual area 4
MT	middle temporal area
TEO	temporal occipital area
TE	temporal area
TF	temporal area TF
TH	temporal area TH
FST	fundus superior temporal area
LIP	lateral intra-parietal area
FEF	frontal eye field

Cortical Sulci

LS	lunate sulcus
POS	posterior occipital sulcus
STS	superior temporal sulcus
IOS	inferior occipital sulcus
AS	arcuate sulcus
LatS	lateral sulcus
CeS	central sulcus
PS	principal sulcus
IPS	intra-parietal sulcus
CaS	calcarine sulcus

Notes

Financial support was provided by the EEC, Quality of Life and Management of Living Resources (QLG3-1999-01064) and the Human Frontier Science Program Organization (HFSP RG0133/2000-B). A.B. was supported by an MRT grant. We thank Colette Dehay for help with experiments, Brice Ronsin, Antoine Guillarme, Luc Renaud and Christel Merrouche for excellent technical assistance, and Ghislaine Clain for animal care.

Address correspondence to Henry Kennedy, Cerveau et Vision INSERM 371, 18 Avenue du Doyen Lépine, 69675 Bron Cedex, France. Email: kennedy@lyon151.inserm.fr.

References

Adams MM, Hof PR, Gattass R, Webster MJ, Ungerleider LG (2000) Visual cortical projections and chemoarchitecture of macaque monkey pulvinar. J Comp Neurol 419:377–393.

Andersen RA, Asanuma C, Essick G, Siegel RM (1990) Corticocortical connections of anatomically and physiologically defined subdivisions within the inferior parietal lobule. J Comp Neurol 296:65–113.

Anderson JC, Binzegger T, Martin KAC, Rockland KS (1998) The connections from cortical area V1 to V5: a light and electron microscopic study. J Neurosci 18:10525–10540.

Baizer JS, Ungerleider LG, Desimone R (1991) Organization of visual inputs to the inferior temporal and posterior parietal cortex in macaques. J Neurosci 11:168–190.

Baleydier C, Morel A (1992) Segregated thalamocortical pathways to inferior parietal and inferotemporal cortex in macaque monkey. Vis Neurosci 8:391–405.

Barbas H (1986) Pattern in the laminar origin of corticocortical connections. J Comp Neurol 252:415–422.

Barbas H, Rempel-Clower N (1997) Cortical structure predicts the pattern of corticocortical connections. Cereb Cortex 7:635–646.

Barone P, Dehay C, Berland M, Kennedy H (1994) Developmental changes in the distribution of acetylcholinesterase in the extrastriate visual cortex of the monkey. Dev Brain Res 77:290–294.

Barone P, Dehay C, Berland M, Bullier J, Kennedy H (1995) Developmental remodeling of primate visual cortical pathways. Cereb Cortex 5:22–38.

Barone P, Dehay C, Berland M, Kennedy H (1996) Role of directed growth and target selection in the formation of cortical pathways: prenatal development of the projection of area V2 to area V4 in the monkey. J Comp Neurol 374:1–20.

Barone P, Berland M, Kennedy H (1998) Changes in convergence underly the developmental remodeling of feedback cortical connections in the monkey. Eur J Neurosci 10(Suppl. 10):422.

Barone P, Batardière A, Knoblauch K, Kennedy H (2000) Laminar distribution of neurons in extrastriate areas projecting to V1 and V4 correlates with the hierarchical rank and indicates the operation of a distance rule. J Neurosci 20:3263–3281.

Batardière A, Barone P, Dehay C, Kennedy H (1998a) Area-specific laminar distribution of cortical feedback neurons projecting to cat area 17: quantitative analysis in the adult and during ontogeny. J Comp Neurol 396:493–510.

Batardière A, Barone P, Berland M, Kennedy H (1998b) Laminar reorganization of feedback projections in the primate somatosensory cortex during development. Eur J Neurosci 10(Suppl. 10):136.

Blakemore C, Vital-Durand F (1981) Postnatal development of the monkey's visual system. Ciba Found Symp 86:152–171.

Blatt GJ, Andersen RA, Stoner GR (1990) Visual receptive field organization and cortico-cortical connections of the lateral intraparietal area (area LIP) in the macaque. J Comp Neurol 299:421–445.

Boussaoud D, Ungerleider LG, Desimone R (1990) Pathways for motion analysis: cortical connections of the medial superior temporal and fundus of the superior temporal visual areas in the macaque. J Comp Neurol 296:462–495.

Boussaoud D, Desimone R, Ungerleider LG (1991) Visual topography of area TEO in the macaque. J Comp Neurol 306:554–575.

Boothe RG, Dobson V, Teller DY (1985) Postnatal development of vision in human and nonhuman primates. Annu Rev Neurosci 8:495–545.

Burkalter A (1993) Development of forward and feedback connections between areas V1 and V2 of human visual cortex. Cereb Cortex 3:476–487.

Colby CL, Duhamel JR, Goldberg ME (1996) Visual, presaccadic, and cognitive activation of single neurons in monkey lateral intraparietal area. J Neurophysiol 76:2841–2852.

Coogan TA, Burkhalter A (1988) Sequential development of connections between striate and extrastriate visual cortical areas in the rat. J Comp Neurol 278:242–252.

Coogan TA, Van Essen DC (1996) Development of connections within and between areas V1 and V2 of macaque monkeys. J Comp Neurol 372:327–342.

Dehay C, Kennedy H (1993) Control mechanisms of primate corticogenesis. In: The functional organisation of the human visual cortex (Gulyas B, Roland P, Ottosson D, eds), pp. 13–27. Oxford: Pergamon Press.

Dehay C, Kennedy H, Bullier J, Berland M (1988) Absence of interhemispheric connections of area 17 during development in monkey. Nature 331:348–350.

Desimone R, Ungerleider LG (1986) Multiple visual areas in the caudal superior temporal sulcus of the macaque. J Comp Neurol 248:164–189.

Distler C, Boussaoud D, Desimone R, Ungerleider LG (1993) Cortical connections of inferior temporal area TEO in macaque monkeys. J Comp Neurol 334:125–150.

Distler C, Vital-Durand F, Korte R, Korbmacher H, Hoffmann KP (1999) Development of the optokinetic system in macaque monkeys. Vision Res 39:3909–3919.

Felleman DJ, Van Essen DC (1991) Distributed hierarchical processing in the primate cerebral cortex. Cereb Cortex 1:1–47.

Felleman DJ, Burkhalter A, Van Essen DC (1997a) Cortical connections of areas V3 and VP of macaque monkey extrastriate visual cortex. J Comp Neurol 379:21–47.

Felleman DJ, Xiao Y, McClendon E (1997b) Modular organization of occipito-temporal pathways: cortical connections between visual area 4 and visual area 2 and posterior inferotemporal ventral area in macaque monkey. J Neurosci 17:3185–3200.

Gattass R, Gross CG, Sandell JH (1981) Visual topography of V2 in the macaque. J Comp Neurol 201:519–539.

Gattass R, Sousa APB, Gross CG (1988) Visuotopic organization and extend of V3 and V4 of the macaque. J Neurosci 8:1831–1845.

Gattass R, Sousa APB, Mishkin M, Ungerleider LG (1997) Cortical projections of area V2 in the macaque. Cereb Cortex 7:110–129.

Gonchar Y, Burkhalter A (1999) Differential subcellular localization of forward and feedback interareal inputs to parvalbumine expressing GABAergic neurons in rat visual cortex. J Comp Neurol 406:346–360.

Hilgetag CC, O'Neill MA, Young MP (2000) Hierarchical organization of macaque and cat cortical sensory systems explored with a novel network processor. Phil Trans R Soc Lond B Biol Sci 355:71–89.

Hubel DH, Wiesel TN (1962) Receptive fields binocular interaction and functional architecture in the cat visual cortex. J Physiol 160:106–154.
Hupé JM, James AC, Payne BR, Lomber SG, Girard P, Bullier J (1998) Cortical feedback improves discrimination between figure and background by V1, V2 and V3 neurons. Nature 394:784–787.
Ishai A, Sagi D (1995) Common mechanisms of visual imagery and perception. Science 268:1772–1774.
Jouve B, Rosenstiehl P, Imbert M (1998) A mathematical approach to the connectivity between the cortical visual areas of the macaque monkey. Cereb Cortex 8:28–39.
Kennedy H, Bullier J (1985) A double-labeling investigation of the afferent connectivity to cortical areas V1 and V2. J Neurosci 5:2815–2830.
Kennedy H, Dehay C (1997) The nature and nurture of cortical development. In: Normal and abnormal development of the cortex (Galaburda AM, Christen C, eds), pp. 25–56. Berlin: Springer Verlag.
Kennedy H, Bullier J, Dehay C (1989) Transient projections from STS to area 17 in the newborn monkey. Proc Natl Acad Sci USA 86:8093–8097.
Kennedy H, Salin P, Bullier J, Horsburgh G (1994) Topography of developing thalamic and cortical pathways in the visual system of the cat. J Comp Neurol 348:298–319.
Kennedy H, Batardière A, Dehay C, Barone P (1997) Synaesthesia: implication for developmental neurobiology. In: Synaesthesia: classic and contemporary readings (Baron-Cohen S, Harrisson J, eds), pp. 243–256. Oxford: Basil Blackwell.
Kennedy H, Barone P, Falchier A (2000) Relative contributions of feedforward and feedback inputs to individual areas. Eur J Neurosc 12(Suppl. 11):489.
Kostovic I, Rakic P (1990) Developmental history of the transient subplate zone in the visual and somatosensory cortex of the macaque monkey and human brain. J Comp Neurol 297:441–470.
Lamme VAF, Roelfsema PR (2000) The distinct modes of vision offered by feedforward and recurrent processing. Trends Neurosci 23:571–579.
Lewis JW, Van Essen DC (2000a) Corticocortical connections of visual, sensorimotor, and multimodal processing areas in the parietal lobe of the macaque monkey. J Comp Neurol 428:112–137.
Lewis JW, Van Essen DC (2000b) Mapping of architectonic subdivisions in the macaque monkey, with emphasis on parieto-occipital cortex. J Comp Neurol 428:79–111.
Lund JS, Lund RD, Hendrickson AE, Bunt AH, Fuchs AF (1975) The origin of efferent pathways from the primary visual cortex of the macaque monkey as shown by retrograde transport of horseradish peroxidase. J Comp Neurol 164:287–304.
Maunsell JHR, Van Essen DC (1983) The connections of the middle temporal visual area (MT) and their relationship to a cortical hierarchy in the macaque monkey. J Neurosci 3:2563–2586.
Mesulam MM, Geula C (1994) Chemoarchitectonics of axonal and perikaryal acetylcholinesterase along information processing systems of human cerebral cortex. Brain Res Bull 33:137–153.
Miyashita Y (1995) How the brain creates imagery: projection to primary visual cortex. Science 268:1719–1720.
Morel A, Bullier J (1990) Anatomical segregation of two cortical visual pathways in the macaque monkey. Vis Neurosci 4:555–578.
Price DJ, Ferrer JMR, Blakemore C, Kato N (1994) Postnatal development and plasticity of corticocortical projections from area 17 to Area 18 in the cats visual cortex. J Neurosci 14:2747–2762.
Rempel-Clower NL, Barbas H (2000) The laminar pattern of connections between prefrontal and anterior temporal cortices in the Rhesus monkey is related to cortical structure and function. Cereb Cortex 10:851–865.
Rockland KS (1997) Element of cortical architecture. Hierarchy revisited. In: Cerebral cortex (Rockland KS, Kaas JH, Peters A, eds), pp. 243–293. New York: Plenum Press.
Rockland KS, Pandya DN (1979) Laminar origins and terminations of cortical connections to the occipital lobe in the rhesus monkey. Brain Res 179:3–20.
Rodman HR (1994) Development of inferior temporal cortex in the monkey. Cereb Cortex 4:484–498.
Rodman HR, Scalaidhe SP, Gross CG (1993) Response properties of neurons in temporal cortical visual areas of infant monkeys. J Neurophysiol 70:1115–1136.
Schall JD, Morel A, King DJ, Bullier J (1995) Topography of visual cortex connections with frontal eye field in macaque: convergence and segregation of processing streams. J Neurosci 15:4464–4487.
Shipp S, Zeki S (1995) Segregation and convergence of specialized pathway in macaque monkey visual cortex. J Anat 187:547–562.
Silverman MS, Tootell RBH (1987) Modified technique for cytochrome oxidase histochemistry: increased staining intensity and compatibility with 2-deoxyglucose autoradiography. J Neurosci Methods 19:1–10.
Sireteanu R, Rieth C (1992) Texture segregation in infants and children. Behav Brain Res 49:133–139.
Smart IHM, Dehay C, Giroud P, Berland M, Kennedy H (2002) Unique morphological features of the proliferative zones and postmitotic compartments of the neural epithelium giving rise to striate and extrastriate cortex in the monkey. Cereb Cortex 12:37–53.
Sporns O, Tononi G, Edelman GM (2000) Theoretical neuroanatomy: relating anatomical and functional connectivity in graphs and cortical connection matrices. Cereb Cortex 10:127–41.
Stanton GB, Deng SY, Goldberg ME, McMullen NT (1989) Cyto-architectural characteristic of the frontal eye fields in macaque monkeys. J Comp Neurol 282:415–427.
Suzuki WA, Amaral DG (1994) Perirhinal and parahippocampal cortices of the macaque monkey: cortical afferents. J Comp Neurol 350:497–533.
Tanaka M, Lindsley E, Lausmann S, Creutzfeldt OD (1990) Afferent connections of the prelunate visual association cortex (areas V4 and DP). Anat Embryol 181:19–30.
Tootell RBH, Silverman MS, De Valois RL, Jacobs GH (1983) Functional organization of the second cortical visual area of primate. Science 220:737–739.
Ungerleider LG, Desimone R (1986) Cortical connections of visual area MT in the macaque. J Comp Neurol 248:190–222.
Van Essen DC, Maunsell JHR, Bixby JL (1981) The middle temporal visual area in the macaque: myeloarchitecture, connections, functional properties and topographic organization. J Comp Neurol 199: 293–326.
Van Essen DC, Newsome WT, Maunsell JHR, Bixby JL (1986) The projections from striate cortex (V1) to areas V2 and V3 in the macaque monkey: asymmetries, areal boundaries, and patchy connections. J Comp Neurol 244:451–480.
Vanduffel W, Payne BR, Lomber SG, Orban GA (1997) Functional impact of cerebral connections. Proc Natl Acad Sci USA 94:7617–20
Webster MJ, Ungerleider LG, Bachevalier J (1991) Connections of inferior temporal areas TE and TEO with medial temporal-lobe structures in infant and adult monkeys. J Neurosci 11:1095–1116.
Webster MJ, Bachevalier J, Ungerleider LG (1994) Connections of inferior temporal areas TEO and TE with parietal and frontal cortex in macaque monkeys. Cereb Cortex 4:470–483.
Woodward JA, Bonett DG, Brecht M-L (1990) Introduction to linear models and experimental design. San Diego, CA: Harcourt Brace Jovanovich.
Young MP (1992) Objective analysis of the topological organization of the primate visual cortical system. Nature 358:152–155.
Zipser K, Lamme VA, Schiller PH (1996) Contextual modulation in primary visual cortex. J Neurosci 16:7376–7389.